The Peripheral-Type Benzodiazepine Receptor and Tumorigenicity: Isoquinoline Binding Protein (IBP) Antisense Knockdown in the C6 Glioma Cell Line †

ARTICLE *in* BIOCHEMISTRY · AUGUST 2005

Impact Factor: 3.02 · DOI: 10.1021/bi050150s · Source: PubMed

12 AUTHORS, INCLUDING:

Gary Weisinger
Tel Aviv Sourasky Medical Center
58 PUBLICATIONS **1,363** CITATIONS
SEE PROFILE

Abraham Weizman
Tel Aviv University
946 PUBLICATIONS **19,792** CITATIONS
SEE PROFILE

Moshe Gavish
Technion - Israel Institute of Technology
193 PUBLICATIONS **5,874** CITATIONS
SEE PROFILE

The Peripheral-Type Benzodiazepine Receptor and Tumorigenicity: Isoquinoline Binding Protein (IBP) Antisense Knockdown in the C6 Glioma Cell Line†

Evgeny Levin,‡ Arumugam Premkumar,§ Leo Veenman,‡ Wilfried Kugler,|| Svetlana Leschiner,‡ Ilana Spanier,‡ Gary Weisinger,⊥ Max Lakomek,|| Abraham Weizman,○ Solomon H. Snyder,# Gavril W. Pasternak,§ and Moshe Gavish*,‡

Rappaport Family Institute for Research in the Medical Sciences, Technion-Israel Institute of Technology, Haifa, Israel, Laboratory of Molecular Neuropharmacology, Memorial Sloan Kettering Cancer Center, New York, Pädiatrie I, Universitätsklinikum Göttingen, Göttingen, Germany, The Endocrine Institute, Tel Aviv Sourasky Medical Center, Tel Aviv, Israel, Geha Mental Health Center, Felsenstein Medical Research Center, Rabin Medical Center, Beilinson Campus, Sackler Faculty of Medicine, Tel Aviv University, Petah Tiqva, Israel, and Department of Neuroscience, Pharmacology and Molecular Sciences and Psychiatry, The Johns Hopkins University School of Medicine, Baltimore, Maryland

Received January 26, 2005; Revised Manuscript Received May 25, 2005

ABSTRACT: Peripheral-type benzodiazepine receptors (PBR) are constituted by three protein components, the isoquinoline binding protein (IBP), the voltage-dependent anion channel (VDAC), and the adenine nucleotide transporter (ANT). Recently, we found that high levels of PBR ligand binding in glioma cell lines correlate with in vitro tumorigenicity. To study whether enhanced PBR expression is causative or in response to cancer, we genetically modified C6 glioma cells. Antisense knockdown of the IBP resulted in more than 50% reductions in PBR ligand binding both in the mitochondrial and whole cell fractions, accompanied by similar reductions in IBP levels in these respective fractions. The IBP knockdown was accompanied by a 25% increase in cell number in confluent cultures. This correlated with an 8-fold increase in in vitro tumorigenicity, as assessed by anchorage independent growth. Cell cycle analysis indicated that knockdown of the IBP resulted in a 60% reduction in the number of cells in the pre-G1 apoptosis phase. This paralleled the reduction seen in apoptosis and cell death shown by DNA fragmentation and Trypan blue assays, respectively. Furthermore, knockdown of the IBP appeared to prevent induction of apoptosis by the antineoplastic agent, erucylphosphocholine. In addition, IBP knockdown prevented processing of the caspase 3 component of the apoptosis cascade by the erucylphosphocholine congener, erucylphospho-*N*,*N*,*N*-trimethylammonium. In conclusion, our results suggest that enhanced IBP expression, including enhanced PBR ligand binding, such as occurring in untreated C6 glioma cells, may provide a mechanism to increase apoptotic rates of cancer cells.

Peripheral-type benzodiazepine receptors (PBR)[1] are heterotrimers composed of three protein components, an isoquinoline carboxamide binding protein (IBP, 18-kDa), a voltage-dependent anion channel (VDAC, 32-kDa), and an adenine nucleotide transporter (ANT, 30-kDa) (*1*). PBR are abundant in peripheral tissues (*2*, *3*) as well as in glial cells in the brain (*4*, *5*) and are located primarily on mitochondrial membranes (*6*−*9*). Topographic analysis of the receptor distribution on the mitochondrial membrane has indicated that a receptor complex is formed by several 18-kDa IBP molecules associated with one VDAC molecule (*10*) and that this complex is located at the contact sites between the outer and inner mitochondrial membranes (*11*). In addition, it appears that the ratio of IBP to VDAC is tissue- and treatment-specific (*12*, *13*). Structurally, VDAC forms the core of a protein complex which, in addition to IBP and ANT, may include proteins of the Bcl-2 family and creatine kinase (*14*−*16*).

† This research was supported by the U.S.-Israel Binational Science Foundation, No. 9800315 (to M.G., A.W., S.H.S.); the National Institute of Drug Abuse, Nos. DA00220 (Senior Scientist Award) and DA06241 (to G.W.P.); and B. Braun-Stiftung (to W.K.). The Center for Absorption in Science, Ministry of Immigrant Absorption, State of Israel, is acknowledged for their support to S.L. and L.V.

* To whom correspondence should be addressed: Professor M. Gavish, Rappaport Family Institute for Research in the Medical Sciences, Technion-Israel Institute of Technology, Department of Pharmacology, P.O.B. 9649, Bat-Galim, Haifa 31096, Israel. Fax: 972-4-8295271. Tel.: 972-4-8295275. E-mail: mgavish@tx.technion.ac.il.

‡ Technion-Israel Institute of Technology.

§ Memorial Sloan Kettering Cancer Center.

|| Universitätsklinikum Göttingen.

⊥ Tel Aviv Sourasky Medical Center.

○ Tel Aviv University.

The Johns Hopkins University School of Medicine.

[1] Abbreviations: ABTS, 2,2′-azino-bis-[3-ethylbenzothiazoline]-6-sulfonic acid; ANT, adenine nucleotide transporter; BSA, bovine serum albumin; CAT, chloramphenicol acetyl transferase; CMV, cytomegalovirus; DDW, double distilled water; DMEM, Dulbecco's Modified Eagle Medium; DTT, dithiothreitol; dNTP, deoxy nucleotide triphosphate, EDTA, ethylenediamine tetraacetic acid; FACS, fluorescence-assisted cell sorting; IBP, isoquinoline binding protein; PBR, peripheral-type benzodiazepine receptors; PBS, phosphate-buffered saline; PBS-T, PBS-Tween 20; PK 11195, 1-(2-chlorophenyl)-*N*-methyl-*N*-(1-methylpropyl)-3-isoquinolinecarboxamide; Ro 5-4864, 4′-Chlorodiazepam; TLC, thin layer chromotography; SDS, sodium dodecyl sulfate; Tris, tris(hydroxymethyl)aminomethane buffer; VDAC, voltage-dependent anion channel; ErPC, erucylphosphocholine; ErPC3, erucylphospho-*N*,*N*,*N*-trimethylammonium.

10.1021/bi050150s CCC: $30.25
Published on Web 06/25/2005

A broad spectrum of putative functions have been suggested for the PBR, such as regulation of steroid production (*17*−*21*), involvement in cell growth and differentiation (*22*−*25*), regulation of the mitochondrial respiratory chain (*26*, *27*), effects on the immune and phagocytic host defense response (*28*, *29*), modulation of voltage-dependent anion channels (*30*), responses to stress (*31*, *32*), microglial activation related to brain damage (*13*, *33*−*35*), and cancer cell proliferation (*21*, *23*, *25*, *36*), including glial tumor cells (*34*, *37*, *38*). Yet, the relative importance of PBR for many of these functions is still unclear (*39*).

Several studies have demonstrated increased binding of PBR ligands in various brain tumors (*34*, *38*, *40*, *41*). This property can be used to accurately delineate glioma borders using positron emission tomography (*42*). For example, in rat, C6 glioma PBR densities are increased up to 30-fold compared to the surrounding neocortex (*38*, *43*). In human post mortem tissue, intact glioma cells presented high levels of PBR ligand binding, while necrotic areas of the tumor and cells in surrounding normal tissue did not display detectable levels of PBR ligand binding (*44*). In addition, tritiated 1-(2-chlorophenyl)-*N*-methyl-*N*-(1-methylpropyl)-3-isoquinolinecarboxamide, [^{3}H]PK 11195, binding in specimens from human gliomas suggested that PBR characteristics may be used to differentiate between high- and low-grade gliomas (*45*). Treatment with the specific PBR ligands, PK 11195 and Ro5 4864 (4′-chlorodiazepam), can induce morphological changes, both in rat C6 and human T98G glioma cells (*46*). Ikezaki and Black (*47*) showed that for rat C6 glioma cells, growth rate and thymidine incorporation increased by 20−30% after PK 11195 exposure in the nanomolar range. Recently, we found that enhanced PBR levels in untreated glioma cells correlate with enhanced tumorigenicity (*48*). In particular, high levels of PBR in untreated glioma cells were correlated with enhanced anchorage-independent growth, increased cell numbers, and reduced levels of apoptosis. Nonetheless, these data could not resolve the exact functional meaning of the relatively high PBR binding levels for tumorigenicity (*48*). In another study, it was shown that MA-10 Leydig cells displaying PBR dysregulation due to IBP antisense knockdown also demonstrated increased tumorigenicity, even though this effect did not seem to be due to changes in the proliferation rate of these cells (*21*, *49*).

We undertook the present study to further clarify whether PBR's role is causative, contributory, or in response to cancer. Therefore, we focused on the effect of IBP antisense knockdown on in vitro tumorigenicity in C6 rat glioma cells indicated by anchorage-independent growth as assessed by their ability to form colonies in soft agar. In addition, we studied the effects on cell number, cell cycle, and apoptosis in regular culture medium to gain insights whether the effects of IBP knockdown involve changes in cell multiplication and/or cell death, including apoptosis. Moreover, we assayed the effects of IBP knockdown on the apoptosis inducing characteristics of the antineoplastic agent erucylphosphocholine (ErPC) and its congener erucylphospho-*N*,*N*,*N*-trimethylammonium (ErPC3). Previously, it was shown that ErPC induces apoptosis in glioma cells by activating the apoptosis cascade including reduction of the mitochondrial membrane potential, cytochrome *c* release, and caspase activation (*50*−*52*). For these aims, we compared ErPC and ErPC3 effects between stable IBP antisense knockdown C6 cells and control C6 cells containing vector without the IBP antisense gene. We found that IBP antisense knockdown reduced basal apoptotic levels, blocked the proapoptic activity of the antineoplastic agent ErPC and caspase 3 processing following ErPC3 treatment of C6 glioma cells, and enhanced tumorigenicity in this cell line.

MATERIALS AND METHODS

Cells and Materials. The C6 glial tumor cell line from rat (glioma) was used as described by the American Type Culture Collection. The cells had been subject to five passages prior to the stable transfection performed in this study. Culture medium for C6 consisted of Dulbecco Modified Eagle Medium (with glucose 4500 mg/L, without sodium pyruvate and L-glutamine) (DMEM), with addition of a 200 mM L-glutamine saline solution (2% v/v). Additionally, fetal calf serum (10% v/v), penicillin−streptomycin solution (10 000 units/mL penicillin sodium salt and 10 mg/mL streptomycin sulfate) (1% v/v), and amphotericin B solution (2.5 mg/mL) (0.1% v/v) were added to the culture media. Culture medium ingredients were obtained from Biological Industries (Beit HaEmek, Israel).

[^{3}H]PK 11195 was obtained from New England Nuclear (Boston, MA). Unlabeled PK 11195 was purchased from Sigma-Aldrich Israel (Israel). The Cell Proliferation Kit (Cell Proliferation Assay with XTT Reagent) was obtained from Biological Industries (Beit HaEmek, Israel). The Cell Death Kit (Cell Death Detection ELISA^{PLUS} Kit) and protease inhibitor was obtained from Roche Molecular Biochemicals (Mannheim, Germany). Nylon mesh (30 μm) for cell separation for the FACS analysis was obtained from Sinun (Petach Tikva, Israel). TriReagent was obtained from MRC (Cambridge, U.K.). Superscript reverse transcriptase, the pcDNA3.0 vector, and Lipofectamine 2000 reagent were obtained from Invitrogen (Paisley, U.K.). The DNA clean kit was obtained from Zymo Research (Orange, CA). Nitrocellulose membrane (Hybond ECL), horseradish peroxidase-linked anti-rabbit IgG, ECL detection reagents, and Hyperfilm were obtained from Amersham Biosciences (Rehovot, Israel). ErPC and its congener ErPC3 were kindly provided by Prof. H. Eibl, Max-Planck-Institut für biophysikalische Chemie, Göttingen, Germany, and synthesized as previously described (*52*).

Standard chemicals were obtained from commercial dealers.

Chloramphenicol Acetyl Transferase (CAT) Assay. To select the most effective promoter for our IBP antisense knockdown study of C6 glioma cells, CAT assays were performed according to the method of Gorman et al. (*53*). In brief, 48 h after lipofection, C6 cells were washed three times with PBS (without Ca^{2+} and Mg^{2+}). Then, the cells were incubated for 5 min with 1 mL of Tris (40 mM)/EDTA (1 mM)/NaCl (150 mM) (pH 7.4) per well. The cells were scraped from the wells, transferred to microtubes, and centrifuged at 1000*g* for 2 min. The pellet was resuspended in 50 μL of lysis buffer (0.25 M Tris-HCl, pH 7.8). The cells were lysed by freeze/thawing: 5 min at −80 °C, followed by 5 min in 37 °C water bath, followed by resuspension with a vortex. The procedure was performed

three times. The cell lysate was centrifuged for 5 min at 10 000*g*, and the supernatant, containing cell extract, was transferred to new microtubes.

Subsequently, the CAT reaction was performed. The reaction ingredients were combined in the following way: 70 μL Tris-Cl (pH 7.8) + 20 μL cell extract + 1 μL [^{14}C]-chloramphenicol (0.1 μCi) + 39 μL DDW. The ingredients were gently mixed and microcentrifuged. This reaction mix was incubated for 5 min at 37 °C prior to the addition of 20 μL of 4 mM Acetyl-CoA (Li salt; 10 mg/2.84 mL H_2O). The reaction was continued for 60 min at 37 °C, terminated, and extracted into 1 mL of ethyl acetate. The phases were separated by a 30 s microcentrifugation (10 000*g*) at 4 °C. The upper organic phase was collected carefully and dried with a Speed-Vac (Savant Instruments, Inc., Farmingdale, NY). The dried residue was dissolved in 25 μL of fresh ethyl acetate and then spotted on a 20 cm × 20 cm silica gel thin layer chromotography (TLC) plate, 1.5 cm from the plate bottom. The plate was then run ascending in a preequilibrated (>30 min) closed glass TLC tank in 95% chloroform/5% methanol (v/v) for 90 min. The air-dried plate was then exposed to a Kodak XAR film at room temperature for 1−5 days, before film development.

RNA Isolation, Reverse Transcription-PCR (RT-PCR), and Cloning of IBP. Total RNA was extracted from rat kidney tissue using TriReagent (MRC), and the quality and quantity were measured with a spectrophotometer. For RT-PCR, about 5 μg DNase-digested total RNA was reverse-transcribed using superscript reverse transcriptase (Invitrogen) following the recommendations of the manufacturer. In brief, 5 μg RNA template and 0.2 μM oligo (dT) primer mixture were incubated at 65 °C for 10 min and then cooled on ice for 2 min. cDNA synthesis was initiated by addition of 1× first strand buffer (Invitrogen), 25 μM dNTPs, 10 mM dithiotheitol (DTT), and 2 U SuperScript II RT RNase H reverse transcriptase (Invitrogen) in a 20 μL reaction volume and incubated at 42 °C for 50 min. Full-length cDNA of IBP was amplified using forward primer (CCTCTAGAATGTCTCAATCCTGGGTACCCG) and reverse primers (GGTCTAGATCACTCTGTGAGCCGGGAGCC) with an XbaI restriction site in both primers. The conditions for PCR were as follows: 3 min at 95 °C, 35 cycles of 1 min at 92 °C, 1 min at 60 °C, and 1.5 min extension at 72 °C. After the cycles, a final extension was carried out at 72 °C for 5 min. The amplified fragment was then purified and cut with Xba I and gel purified using DNA clean kit (Zymo Resarch). The XbaI-digested fragment was cloned into pcDNA3.0 vector (Invitrogen). Antisense IBP clones were selected by restriction analysis and DNA sequencing.

Transfection. For transfection, 2 μg of plasmid DNA (pcDNA3.0), containing antisense IBP cDNA to prepare IBP knockdown clones, or plasmid DNA, without the antisense IBP gene to prepare control cells, was mixed individually with 6 μL Lipofectamine 2000 reagent (Invitrogen) in 0.5 mL of serum-free DMEM medium. Approximately 60−70% confluent C6 glioma cells were transfected with the mixture and incubated for 10 h. Then, the transfection medium was replaced with fresh DMEM containing 10% fetal calf serum and 800 μg/mL G418 (a stable analogue of neomycin; Calbiochem, Darmstadt, Germany), and the stable clones were selected by the presence of G418 for 2−3 weeks. Individual colonies transfected with antisense IBP cDNA were picked up by using pipet tips, and the cells were amplified. IBP knockdown clones were selected by binding with [^{3}H]PK 11195 and used for further detailed assays of relative levels of [^{3}H]PK 11195 binding, IBP levels, tumorigenicity, cell viability, and apoptotic processes. Mixed colonies of cells transfected with the plasmid DNA without the antisense IBP gene (vector plasmid) were used as control cells for all the assays applied in this study.

PBR Ligand Binding. [^{3}H]PK 11195 binding values were assessed in IBP knockdown clones and control cells that were confluent for 5 days. To collect whole cells for the binding assay, the stably transfected cells were scraped from the flasks in their culture medium. The cells were centrifuged (1000*g*, 10 min), resuspended in 1 mL of medium, and centrifuged (1000*g*, 10 min). The pellets were snap-frozen in liquid nitrogen and stored at −70 °C until further use. For further processing, the pellet was thawed and homogenized in 3 mL of phosphate-buffered saline (PBS) using a Kinematika Polytron (setting 6) for 10 s and centrifuged at 37 000*g* for 30 min. The pellet was then resuspended in 1 mL of PBS, homogenized, and centrifuged, as above. The pellet again was resuspended in 1 mL of PBS. The mitochondrial fraction was prepared as described below for the Western blot analysis, however, with omission of solubilization with sodium dodecyl sulfate (SDS). Protein content was determined by the method of Bradford (*54*) using bovine serum albumin (BSA) as a standard. Binding of [^{3}H]PK 11195 to the whole cell and mitochondrial membranes of the clones stably transfected with the plasmid containing the IBP antisense cDNA (IBP knockdown clones) and the cells stably transfected with the vector plasmid (control cells) was conducted, as previously described (*21*, *25*, *48*, *49*, *55*). The reaction mixture contained 400 μL of the homogenized membranes in question (40 μg protein) and 25 μL of [^{3}H]-PK 11195 solution (final concentration, 6 nM) in the absence (total binding) or presence (nonspecific binding) of 75 μL unlabeled PK 11195 (10 μM final concentration) for one-point binding analysis. After incubation for 60 min at 4 °C, the samples were vacuum-filtered through Whatman GF/C filters, washed three times with 4 mL phosphate buffer, and placed in vials containing 4 mL of Opti-Fluor. Radioactivity was counted after 12 h with a 1600CA Tri-Carb liquid scintillation analyzer (Packard, Meriden, CT).

Whole Cell Extract Preparation for Western Blot Analysis. Whole cell extracts of IBP knockdown clones and control cells were used for Western blot analysis as previously described (*48*). Briefly, flasks with cultured, stably transfected cells confluent for 5 days were washed three times with PBS. Then, the cultured cells were scraped into 500 μL of PBS. The samples were centrifuged at 1000*g* for 6 min. The cell pellets were lysed with 200 μL of lysis buffer containing 1% Triton X-100, 1 tablet/10 mL of protease inhibitor (Roche), and 0.1% SDS dissolved in PBS, pH 7.4, for 30 min at 4 °C. Subsequently, the samples were centrifuged at 10 000*g* for 10 min at 4 °C. Then, the supernatants were transferred to microtubes. Protein levels were measured by the method of Bradford (*54*). The samples were aliquoted and frozen at −80 °C.

Mitochondrial Fraction Preparation for Western Blot Analysis. Mitochondrial fractions of IBP knockdown and control cells were used for Western blot analysis, according to methods described previously (*13*). Briefly, the adherent,

stably transfected cells were washed with PBS, scraped into 500 μL of PBS, and centrifuged 1000*g* for 6 min. The pellet was resuspended in lysis buffer B containing 1mM EDTA, 250 mM sucrose, 5 mM Tris-HCl (pH 7.5) and protease inhibitor (Roche) and was incubated for 15 min on ice. The lysate was homogenized with a glass homogenizer (20 strokes) and incubated for 5 min, and 20 strokes more were performed. The cell lysate was centrifuged at 1000*g* for 10 min, and the supernatant containing the mitochondrial fraction was transferred into a new microtube. Then, the supernatant was centrifuged at 13 000*g* for 20 min, and the pellet was resuspended with buffer B and again centrifuged at 13 000*g* for 20 min. This procedure was performed one more time. For Western blot analysis, SDS was added to a final concentration of 1%, and the samples were centrifuged at 10 000*g* for 10 min. The protein quantity of the supernatant was measured according to the method of Bradford (*54*), and the samples were frozen in −80 °C.

Western Blot Analysis. Western blot protein analysis was performed according to methods described previously (*12*, *13*, *52*). Briefly, samples of whole cell extracts or mitochondrial fractions (solubilized with 1% of SDS and frozen at −80 °C) were thawed and prepared in 2× sample buffer (0.125 M Tris-HCl (pH 6.8), 20% glycerol, 4% (w/v) SDS, 0.14 M β-mercaptoethanol, and 0.0005% (w/v) bromophenol blue). The samples were boiled for 10 min and subjected to electrophoresis through 12% SDS−polyacrylamide gel (10−20 μg protein/lane). The protein extracts were then electrophoretically transferred to nitrocellulose membrane (Hybond ECL, Amersham) in 20 mM Tris-HCl, 150 mM Glycine, and 20% methanol for 1 h at 100 W, followed by blocking of the membrane in 5% dried milk (Carnation, Glendale, CA) in PBS-T (PBS containing 0.1% Tween 20). After several washes, the membranes were incubated with a primary antibody (for example, polyclonal anti-18 kDa IBP antibody prepared in the laboratory of M. Gavish) in 1% dried milk in PBS-T for 2 h. The membranes were washed in PBS-T followed by a 1 h incubation with the secondary antibody (horseradish peroxidase-linked anti-rabbit IgG, from Amersham). After washing the blot with PBS-T, the membrane was incubated for 1 min with ECL detection reagents (Amersham) and exposed to Hyperfilm (Amersham) for 30−60 s. Relative intensities of the Western blot labeling of the 18-kDa IBP and the other proteins of interest, extracted from the IBP knockdown clones and control cells, were determined densitometrically utilizing Biocapt-[Biocap1] Version 97.05 s for Windows and Bio-Profile, Bio-1D, Windows, Application V97.04 (Vilber Lourmat, France).

To assay caspase 3 processing, a monoclonal rabbit anti-caspase 3 antibody (1:1000; Cell Signaling, Frankfurt, Germany) was used as described previously (*52*). To verify protein loading, the blots were stripped with 62.5 mM Tris (pH 6.8), 2% SDS, and 100 mM β-mercaptoethanol for 10 min at 60 °C and reprobed with a polyclonal rabbit antibody against p44/42 MAP kinase (ERK) (1:50 000; Sigma).

Cell Growth in Soft Agar. This assay was performed as previously described (*48*, *49*). Briefly, Bacto Agar was used to prepare a solution of 0.6% agar in culture medium. To each 25 cm^2 plate, 6 mL of the 0.6% agar solution was added and allowed to solidify for 24 h at room temperature. A 0.3% agar solution was prepared by mixing half of one part of 2× concentrated medium, one-quarter part of sterile double distilled water, 3×10^4 cells per cell line (individual IBP knockdown clones and control cells), and one-quarter part of a 1.2% agar solution warmed to 48 °C. Of this mixture, 1.5 mL was added on top of the agar in the prepared wells. In these wells, the cells were allowed to proliferate for 21 days. For analysis of colony size, a Zeiss Axioscop 2 inverted microscope and Image ProPlus software version 4.5.1.25 for Windows was used. Briefly, the wells were subdivided in 16 approximately equally sized areas, and from the centers of five such subdivisions, the square measures of the observed colonies were determined. In addition, cell numbers per colony were counted, and the colonies were categorized into three groups, less than 100 cells per colony, 100−300 cells per colony, and greater than 300 cells per colony, using a standard inverted microscope.

Cell Number and Cell Death Assays. Cell counts were performed for IBP knockdown clones and control cells growing in regular medium, as described previously (*48*, *49*). Briefly, cell number and the percentage of cell death for stably transfected cells were calculated with the aid of a hemocytometer 5 days after having reached 100% confluency, since at this stage PBR expression, as determined by ligand binding, appeared to be stable (*48*). Then, the medium covering the cells was collected, the cells were trypsinized and added to the collected medium, and a sample was taken for cell counting. The cells were counted visually using an inverted microscope (Olympus CK2) with the aid of a hemocytometer. To determine the percentage of dead cells, cells were stained with Trypan blue at a final concentration of 0.25%.

Apoptosis. To determine differences in apoptosis between IBP knockdown clones and control cells, we used the Cell Death Kit, as described previously (*48*). For this programmed cell death assay, 4×10^5 cells were seeded and counted as described by the manufacturer. A fraction of the suspension containing 10^6 cells was centrifuged (1000*g*, 5 min), the pellet was resuspended in 1 mL medium, centrifuged (1000*g*, 5 min), and the pellets were snap-frozen in liquid nitrogen and stored at −70 °C until use. Upon apoptosis analysis, the cell pellets were allowed to thaw and then resuspended with lysis buffer according to the manufacturer's instructions. The lysate was centrifuged at 200*g* for 10 min. A fraction of the supernatant was transferred to streptavidin-coated microtiter plate modules. Immunoreagent was added (anti-histone-biotin and anti-DNA-peroxidase in incubation buffer), and after incubation with gentle shaking for 2 h, the modules were rinsed three times with incubation buffer. Then, the signal for apoptosis was measured following incubation for 20 min with 2,2′-azino-bis-[3-ethylbenzothiazoline]-6-sulfonic acid (ABTS) solution, according to the manufacturer's instructions. The level of staining by the ABTS substrate was determined with an ELISA reader, at the wavelength of 405 nm. Reference absorbance was measured using a 490 nm wavelength. The ABTS solution by itself was used as a blank.

Flow Cytometric Analysis (FACS). Fluorescence-assisted cell sorting (FACS) was used to monitor the cell cycle profile of the IBP knockdown clones and the control cells, according to methods described previously (*25*, *48*, *56*). Briefly, 4×10^5 stably transfected cells were seeded in 25 cm^2 flasks, and the cells were allowed to grow for 5 more days after having reached 100% confluency. Then, the medium cover-

ing the cells was collected, and the cells were trypsinized and added to the collected medium. The cell suspension was centrifuged (300*g*, 5 min), and the pellet was resuspended in 1 mL of PBS and centrifuged at 4 °C. Then, each cell pellet was resuspended in 400 μL of a 70% ethanol solution and incubated for 1 h at 20 °C. Then, 600 μL PBS was added to each suspension and mixed, followed by centrifugation (1000*g*, 6 min) at 4 °C. The pellets were resuspended and incubated in 500 μL PBS containing 100 μg/mL RNAase and 0.5% Triton X-100 for 30 min at 37 °C. Then, propidium iodide was added to a final concentration of 100 μg/mL for an incubation of 10 min at 4 °C to stain the cell nuclei. Then, the cells were filtered through a (30 μm) nylon mesh and vortexed just before FACS analysis on a FACScan (Becton Dickinson, Mountain View, CA). Routinely 20 000 cells were collected per assay point. Data were analyzed by the CellQuest software package (BD, Franklin Lakes, NJ).

Apoptosis Induction and Caspase 3 Processing with Erucylphosphocholine. IBP knockdown clones and control cells were seeded in 24 well plates. Treatment of cells with ErPC commenced 2 days after the cells having attained confluency. A stock solution of 10 mM ErPC was prepared as described previously (*50*). The treatment of the C6 IBP knockdown cells and control cells consisted of application for 2 days of 100 μM ErPC or equal amounts of vehicle per 2 mL medium per well. The medium of treatment was refreshed once after 1 day of the initial application of ErPC and vehicle. Apoptotic rates were determined with the Cell Death Kit as described above. Apoptotic levels of the vehicle-treated cells were taken as standards to which the apoptotic levels of the equivalent ErPC-treated cells were compared.

For assays of caspase-3 processing, whole-cell detergent extracts were prepared from the different C6 clones treated with 100 μM ErPC3 for 72 h or left untreated as described (*52*). Western blot analysis for caspase 3 processing was performed as described above.

Statistical Analysis. For statistical analysis, experimental and control groups were with $n \geq 5$. Results are presented as means ± SD. Student's *t* test analysis was used to determine significant differences between experimental and control groups. When appropriate, one-way analysis of variance (ANOVA) was carried out with the Student−Newman−Keuls post-hoc test. When standard deviations differed significantly between groups, as indicated by Bartlett's test for homogeneity of variance, the nonparametric Kruskal−Wallis test, followed by the Dunn's Multiple Comparison post-hoc test was used. $P < 0.05$ was considered statistically significant (*57*).

RESULTS

IBP Antisense Knockdown in the C6 Glioma Cell Line. To determine the most effective promoter/enhancer for C6 glioma cells for our use in plasmid design and construction, CAT promoter/enhancer assays were performed. These assays led us to use the pcDNA3.0 plasmid vector to clone the full-length 18-kDA IBP downstream of the CMV promoter/enhancer (Figure 1).

Stable IBP antisense cDNA transfections to prepare IBP knockdown clones and stable vector plasmid transfections to prepare control cells were carried out in C6 glioma cell line, as described in Materials and Methods. In the first stage of the analysis of antisense and control stable transfectant cell clones, PBR ligand binding assays using [^{3}H]PK 11195 as a measure of the efficiency of IBP knockdown were performed on whole cell extracts prepared from the IBP

Table 1: Whole Cell Extract Binding (*B*) Values (fmol/mg Protein) of [^{3}H]PK 11195 of IBP Knockdown Clones Compared to That of Plasmid Control Cells (Transfected with Vector Plasmid)[a]

cells	mean *B* value ± standard deviation (fmol/mg protein)
control cells	2168 ± 626
IBP knockdown clones	842 ± 259 ($p < 0.01$)

[a] The mean [^{3}H]PK 11195 binding value of the control cells stems from seven different flasks. The mean [^{3}H]PK 11195 binding value of IBP knockdown clones stems from six flasks of the IBP knockdown clones, i.e., one flask for each IBP knockdown clone.

Table 2: Whole Cell Extract Binding (*B*) Values (fmol/mg Protein) of [^{3}H]PK 11195 for the Individual IBP Knockdown Clones, Referenced to the Mean *B* Value of the Control Cells (Transfected with Vector Plasmid)[a]

cells	*B* value (fmol/mg protein)
control cells	2168
3.1 AS	1133
3.2 AS	1205
3.3 AS	585
3.4 AS	687
3.6 AS	710
3.7 AS	734

[a] Average [^{3}H]PK 11195 binding value of the control cells (see Table 1) and one sample for each IBP knockdown clone (no. AS).

Table 3: Average Mitochondrial PBR Binding (*B*) Values (fmol/mg Protein) of [^{3}H]PK 11195 of IBP Knockdown Clones Compared to That of Control Cells (Transfected with Vector Plasmid)[a]

cells	mean *B* value ± standard deviation (fmol/mg protein)
control cells	4335 ± 1328
IBP knockdown clones	1912 ± 975 ($p < 0.01$)

[a] Six separate clones provided the mean *B* value ± standard deviation of the [^{3}H]PK 11195 binding of the IBP knockdown clones, with each individual number presenting the average of quadruple measurements of one IBP knockdown clone. The mean *B* value ± standard deviation of [^{3}H]PK 11195 binding of the control cells resulted from six averaged quadruple measurements.

Table 4: Mitochondrial Binding (*B*) Values (fmol/mg Protein) of [^{3}H]PK 11195 of Individual Knockdown Clones (No. AS), Referenced to the Average *B* Value of the Control Cells (Transfected with Vector Plasmid)[a]

cells	mean *B* value ± standard deviation (fmol/mg protein)
control cells	4335 ± 1328
3.1 AS	3634 ± 1975
3.2 AS	1653 ± 264
3.3 AS	2079 ± 517
3.4 AS	1569 ± 389
3.6 AS	1876 ± 1436
3.7 AS	658 ± 628

[a] Average [^{3}H]PK 11195 binding value of the control cells (see Table 3) and the average of the quadruple measurements of the *B* value of each IBP knockdown clone.

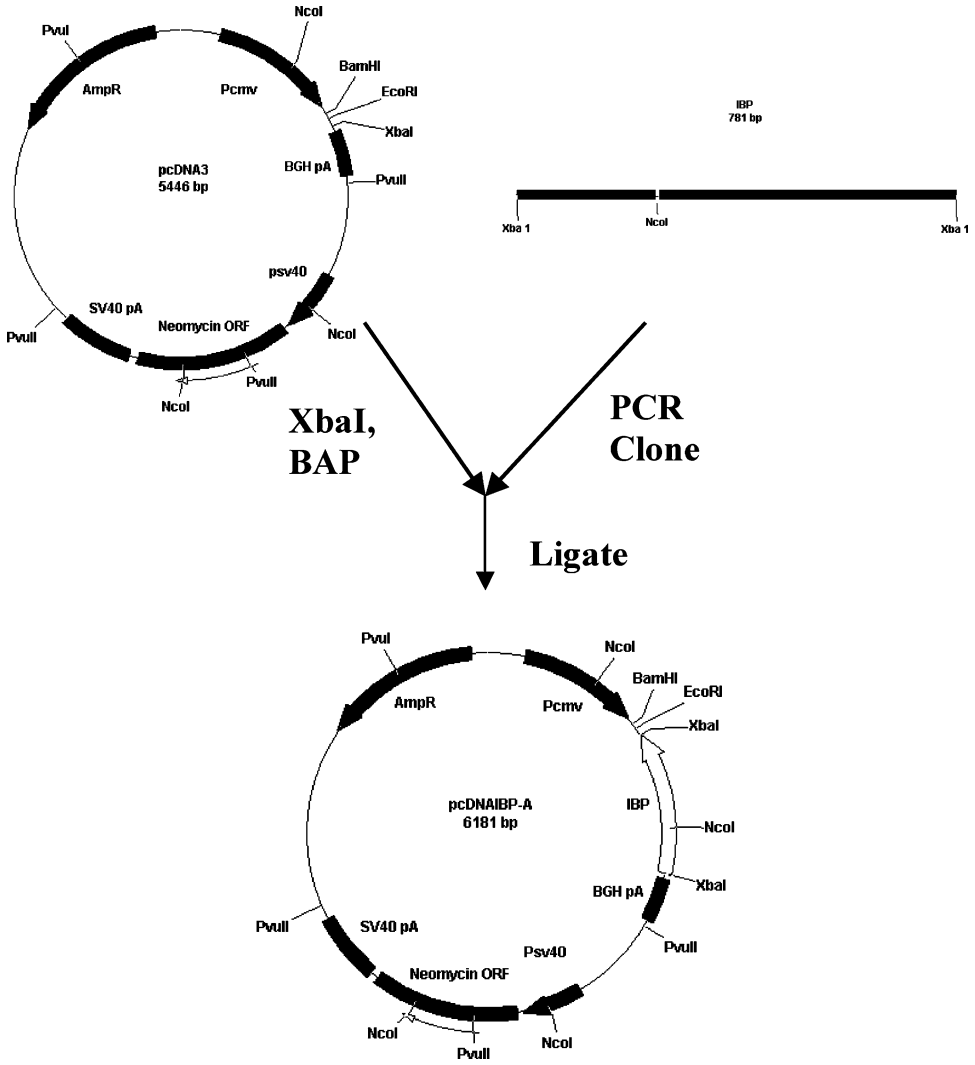

FIGURE 1: CMV-driven IBP antisense knockdown vector construct. The antisense knockdown vector was prepared by subcloning of the full-length IBP cDNA fragment into the EcoRI-cut pcDNA3.0 plasmid in the antisense orientation with respect to the CMV promoter/enhancer.

Table 5: Average PBR Binding and IBP Levels of IBP Knockdown Clones of Mitochondrial Fractions and Whole Cell Extracts Expressed as Percentage of Their Respective Controls (Cells Transfected with Vector Plasmid)

IBP knockdown clones	PBR binding	IBP levels
mitochondrial fractions	44%	69%
whole cell extracts	39%	42%

antisense transfected clones and vector plasmid transfected cells. In this test, a more than 2-fold reduction ($p < 0.01$) of PBR ligand binding in the antisense clones (IBP knockdown clones) compared to the vector plasmid transfected cells (control cells) was seen (Table 1). Each individual IBP knockdown clone showed this range of reduction in PBR ligand binding with [^{3}H]PK 11195 (Table 2). In a previous study, saturability of PBR ligand binding in C6 was demonstrated (*48*).

We also measured PBR binding in mitochondrial extracts. A more than 2-fold reduction ($p < 0.01$) of PBR ligand binding in the IBP knockdown clones compared to the control cells was observed (Table 3). This reduction was comparable to that seen in whole cell extracts (Tables 1 and 5). Table 4 shows that each IBP knockdown clone displayed a lower level of mitochondrial PBR ligand binding in comparison to the control cells. For most IBP knockdown clones, this reduction was more than 2-fold, with the exception of clone 3.1, which showed a 16% reduction in mitochondrial PBR ligand binding (Table 4). Therefore, we decided to continue our study with all individual IBP knockdown clones as one mixed group versus control cells, to average out nonspecific transfection effects as they may occur in our various assays.

Assessment of IBP Protein Level by Western Blot Analysis. We also applied Western blot analysis of whole cell extracts and mitochondrial fractions to measure changes in IBP protein levels as a consequence of IBP knockdown. We found (Figure 2A) that the IBP knockdown clones showed a more than 2-fold reduction in the 18-kDa IBP protein quantity compared to the control cells, in whole cell extracts ($p < 0.01$) (Table 5). In addition, we found a 31% reduction of IBP protein quantity in the IBP knockdown clones compared to control cells for mitochondrial fractions (Figure 2B) (Table 5). This difference was statistically highly significant ($p < 0.001$).

Protein levels of the 36 and 72 kDa polymers of the 18 kDa IBP did not differ between control cells and IBP knockdown clones in whole cell extracts (data not shown).

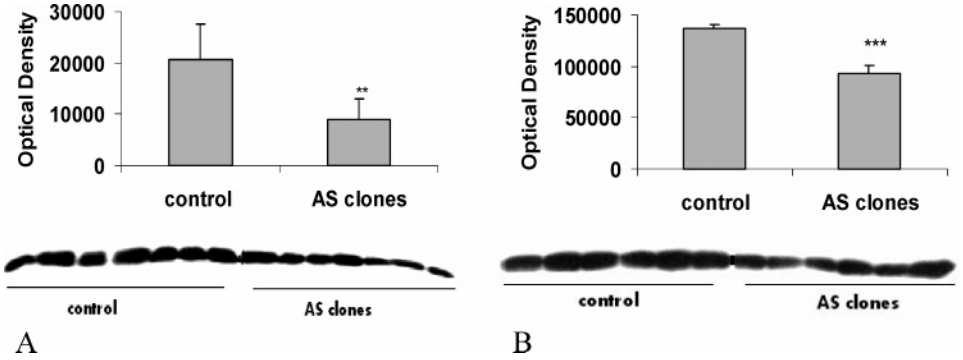

FIGURE 2: Western blot analysis of 18-kDa IBP following antisense knockdown. (A) Differences in IBP levels of whole cell extract between IBP knockdown clones (AS) and control cells (control) are very significant (**, $p < 0.01$). (B) Differences in IBP levels of the mitochondrial fraction between antisense clones and control cells are highly significant (***, $p < 0.001$). The optical density of the labeled 18-kDa bands is presented in arbitrary units.

These average protein levels of 36 and 72 kDa only reached 9% and 8% of the 18-kDa IBP levels, respectively, in control cells. The VDAC protein levels in the mitochondrial fractions also did not differ between control cells and IBP knockdown clones (data not shown), indicating that the observed changes in 18-kDa IBP levels in IBP knockdown clones were specific. These data validated the reduced 18-kDa IBP levels in IBP knockdown clones compared to control cells and are comparable to the reduction in the binding of the isoquinoline PK 11195 (Table 5).

In Vitro Tumorigenicity of the IBP Antisense Clones. In vitro tumorigenicity of IBP knocdown clones versus control cells was determined by measuring anchorage-independent colony growth. We found that IBP knockdown clones grew better in soft agar, since the average area per colony of IBP knockdown clones was significantly larger than that of control cells (approximately 8-fold, $p < 0.01$, Figure 3A,C,D). In addition, IBP knockdown clones produced significantly more colonies and more cells per colony than control cells (Figure 3B,C,D). In particular, they displayed significantly larger numbers of small colonies ($p < 0.05$), medium colonies ($p < 0.005$), and large colonies ($p < 0.05$). Hence, there seems to be an inverse correlation between PBR binding levels and IBP expression on one hand and cell tumorigenicity on the other hand.

Cell Number of Transfected C6 Cell Line. We then evaluated differences in cell number of control cells versus IBP knockdown clones after they had been confluent for 5 days. As depicted in Figure 4, the IBP knockdown clones showed 25% more cells than control cells ($p < 0.05$).

Cell Cycle Analysis of Stably Transfected C6 Cell Lines. We next chose to assess changes in the cell cycle phases of the IBP knockdown clones in comparison to control cells (Figure 5A), as well as to measure changes occurring in the pre-G1 phase (DNA fragmentation) (Figure 5B). Note that the pre-G1 phase is displayed separately, since its measured number of events is much smaller than of the other phases. This correlates with the low level of apoptosis of C6 cells determined in this and a previous study (*48*). We found a lower percentage of IBP knockdown clones in the G1 phase and a larger percentage of the same clones in the G2-M phases in comparison to the control clones (Figure 5A). Differences between S phases of the control cells and IBP knockdown clones were not found. Significantly, there were 2.5-fold less antisense clones in the pre-G1 phase than control cells (Figure 5B). All of these differences were significant

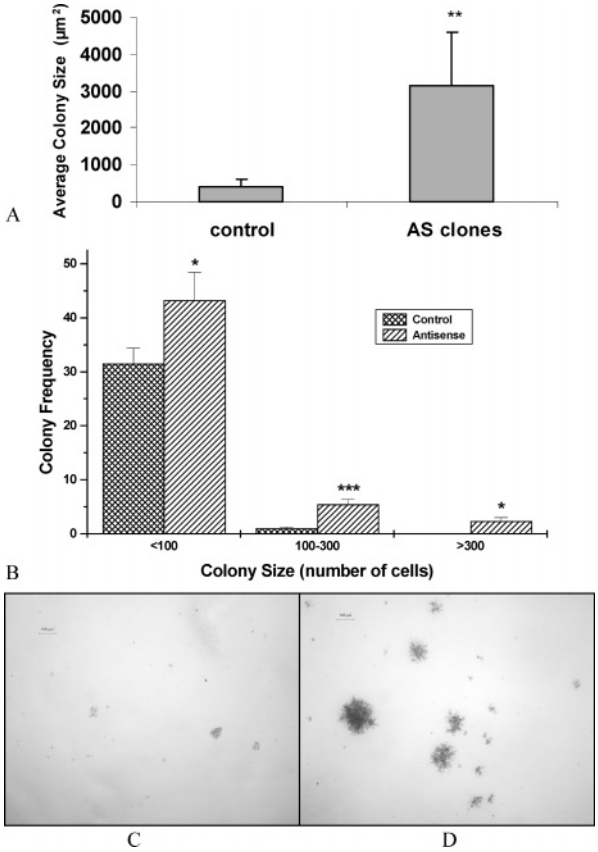

FIGURE 3: Colony growth of IBP knockdown clones in soft agar as an indication of tumorigenicity. (A) Differences in average IBP knockdown clone (AS clones) colony size versus control cells (control) growing in soft agar (**, $p < 0.01$). (B) Numbers of colonies consisting of small (<100), medium (100−300), and large numbers (>300) of cells. IBP knockdown clones (antisense) produce significantly larger numbers of colonies than control cells (control) in each category (small, * $p < 0.05$; medium, ***, $p < 0.005$; large, *, $p < 0.05$). (C and D) Micrographs of control cells (C) and IBP knockdown clones (D) growing in soft agar. These data indicate that the down regulation of IBP by genetic manipulation results in significantly greater in vitro tumorigenicity.

($p < 0.001$). This suggests that the IBP knockdown clones displayed less apoptosis than control cells.

Cell Death Assessed by Measuring Trypan Blue Exclusion and by the Cell Death Kit Assay. Trypan blue staining demonstrated a 2-fold lower percentage of cell death in antisense clones in comparison to the control cells (Figure 6A). This difference was statistically significant ($p < 0.05$).

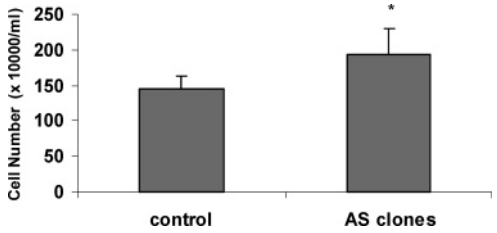

FIGURE 4: Differences in cell number between IBP knockdown clones and control cells 5 days after having reached confluency. Cell number counted with aid of a hemocytometer. IBP knockdown clones versus control cells (*, $p < 0.05$).

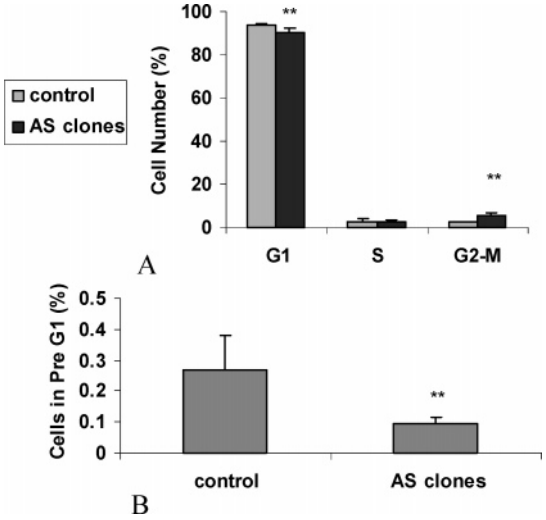

FIGURE 5: Cell cycle analysis by FACS. (A) Differences in percentages of G1 and G2-M phases between IBP knockdown clones (AS clones) and control cells (control) are small but very significant (**, $p < 0.01$). (B) The percentage of IBP knockdown clones (AS clones) in the Pre-G1 phase (DNA fragmentation) is more than 2-fold higher than of control cells (control) (**, $p < 0.01$, very significant).

Basal apoptosis, as measured by the Cell Death Kit assay, showed more than 2-fold lower levels of apoptosis in the IBP knockdown clones in comparison to control cells ($p < 0.001$, Figure 6B). Hence, these data show lower levels of cell death in IBP knockdown clones compared to control cells and corroborate our data from FACS analysis.

Modulation of the Apoptotic Effects of ErPC by IBP Knockdown. Treatment with ErPC caused a 7- to 8-fold increase in apoptotic levels in our control cells (Figure 7). This is comparable to results presented in previous reports (*50*−*52*). Knockdown of the IBP component of the PBR complex in the C6 glioma cell line completely prevented this increase in apoptosis induced by the antineoplastic agent, ErPC (Figure 7; $p < 0.01$).

Effect of IBP Knockdown on Caspase 3 Processing during ErPC3 Treatment. We analyzed whether procaspase 3 was cleaved in IBP knockdown cells in response to ErPC3. The results in Figure 8 indicate that procaspase 3 is readily processed in ErPC3-treated control cells shown by the decrease in the intensity of the full-length protein. This is indicative of caspase 3 activation and comparable to results presented earlier (*50*−*52*). Knockdown of the IBP component of the PBR complex in the C6 glioma cell line almost completely prevented this decrease in procaspase 3 levels induced by the antineoplastic agent ErPC3 (Figure 8). This suggests that the reduction in apoptosis seen in IBP knockdown clones involves a reduction in caspase 3 activation.

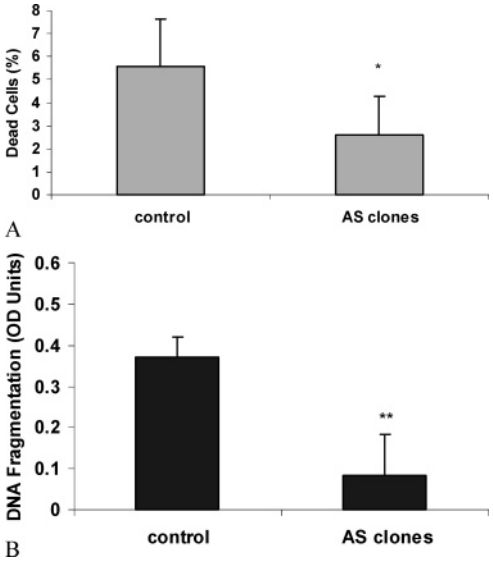

FIGURE 6: Differences in cell viability between IBP knockdown clones (AS) and control cells (control). (A) The percentage of trypan blue positive dead cells among the total number of cells is more than twice as high for IBP knockdown cells, compared to control cells (*, $p < 0.05$). (B) DNA fragmentation as a measure of apoptosis, detected by the Cell Death Kit assay, is also more than twice as high for IBP knockdown cells, compared to control cells (**, $p < 0.01$).

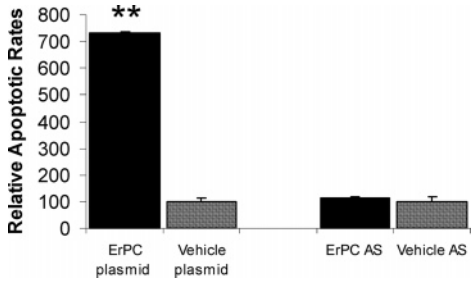

FIGURE 7: Effect of IBP knockdown on apoptosis induction by the antineoplastic agent, ErPC. Apoptotic rates are standardized to 100 arbitrary units in the vehicle-treated cells. The apoptotic rates in the ErPC-treated cells are scaled in respect to their vehicle controls. In control cells (plasmid), ErPC (10^{-4} M), increased apoptotic levels in the C6 glioma cell line 7- to 8-fold compared to baseline level (vehicle). In the IBP knockdown cell line (AS), this apoptotic effect of ErPC was completely abolished. Explanation of abbreviations: "ErPC", treatment with ErPC; "vehicle", treatment with the carrier solution of ErPC (the control treatment); "plasmid", parent vector transfected C6 glioma cells (the control cells); "AS", IBP antisense knockdown C6 glioma cells, the subject of our study. (**, $p < 0.01$, i.e., very significantly different from the corresponding vehicle control group).

DISCUSSION

In a previous study (*48*), we found a correlation between PBR ligand binding density expressed naturally in glioma cell lines and in vitro tumorigenicity. In the current study, we used genetically modified C6 cells that underexpress the 18-kDa IBP to investigate whether PBR ligand binding density may be causative, contributory, or in response to tumorigenicity. Underexpression (knockdown) was achieved by stable transfection of C6 cells with vector plasmids capable of synthesizing antisense 18-kDa IBP mRNA. The mechanism leading to IBP underexpression would involve

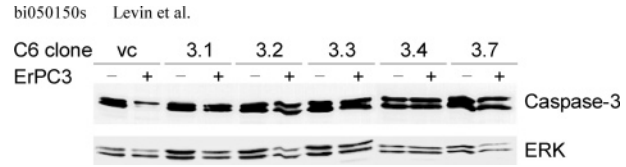

FIGURE 8: Effect of IBP knockdown on caspase 3 processing following treatments with the ErPC3 congener, ErPC3. Control cells (vc) and IBP knockdown clones were cultured in the presence (+) or absence (−) of 100 μM ErPC3 for 72 h. The cells were then lysed, and caspase 3 processing was analyzed by Western blot analysis using a rabbit monoclonal antibody. Protein loading was verified by reprobing for p44/42 MAP kinase (ERK). Explanation of abbreviation and acronyms: "C6 clone" marks the row indicating the cell types used; "vc" is vector control, i.e., parent vector transfected C6 glioma cells (the control cells); "3.1, 3.2, 3.3, 3.4, 3.7", the IBP knockdown clones used for this assay; "ErPC3" marks the row indicating treatment with ErPC3 (+) or its vehicle (−); "caspase-3" marks the row indicating the level of procaspase 3 after treatment with ErPC3 or its vehicle; "ERK" marks the row indicating the levels of the reference protein, P44/42 MAP kinase.

exogenous IBP antisense RNA hybridizing with endogenous 18-kDa IBP mRNA and hence preventing 18-kDa IBP translation. For control, the vector plasmids were stably transfected into C6 cells. This method has already been successfully applied in our laboratory in MA-10 Leydig cells (*21*, *49*).

PBR ligand binding using the tritiated isoquinoline, [^{3}H]-PK 11195, was applied to determine whether C6 cells, stably transfected with the IBP knockdown vector, would express reduced 18-kDa IBP levels. Indeed, more than 50% reductions in the binding of [^{3}H]PK 11195 were observed in both the whole cell extracts mitochondrial fraction of the cell expressing the antisense knockdown vector compared to the cells transfected with control vector (Tables 1−5). As [^{3}H]-PK 11195 binding directly correlates with the number of active IBP sites, our data indicated that we indeed produced C6 IBP antisense knockdown cells.

In addition, we performed Western blot analysis, which would verify if it was possible to see similar differences in 18-kDa IBP protein levels by comparison of IBP knockdown clones and control cells. In particular, we found a more than 50% reduction in whole cell 18-kDa IBP protein levels and a more than 30% reduction in 18-kDa mitochondrial protein levels in IBP knockdown clones compared to control cells, respectively (Table 5). These reductions in 18-kDa IBP levels appeared to be specific, since our results indicated that VDAC protein levels in the mitochondrial fractions were not affected, neither were 36-kDa nor 72-kDA IBP levels in the whole cell extracts (*58*). So, according to PBR ligand binding assays and Western blot analysis, we can conclude that reduction of IBP level was successfully achieved by the current approach. In the present study, we show that IBP knockdown may lead to reduced PBR ligand binding density. In a previous study, we showed that enhanced IBP expression may lead to enhanced PBR ligand binding density (*13*). Thus, IBP levels appear to be positively related to PBR ligand binding density both in vitro and in vivo.

Many biological functions are attributed to the PBR. In recent years, more attention has focused on its regulation of cell proliferation, as a large number of brain tumors and other neoplastic tissues were shown to express higher levels of PBR ligand binding densities than untransformed control tissues (*25*, *36*, *38*, *40*, *41*, *59*, *60*). Moreover, several investigators have found that PBR-specific ligand treatments can also modulate cell proliferation in some of these cells (*23*, *25*, *36*). In the present study, the main aim was to find whether changes in PBR ligand binding were indirect results of cellular transformation or, in fact, were associated with the cause of this pathology.

We previously have shown a correlation between PBR ligand binding density and in vitro tumorigenicity in unmanipulated glioma cell lines (*48*). Another study by us suggested that IBP antisense knockdown in MA 10 cells significantly enhanced tumorigenicity (*49*). We found similar results in colorectal cancer cells (unpublished results). In the current study, we intended to test whether genetic manipulations of PBR expression were able to affect the C6 cells' ability to form colonies in a soft agar matrix. Anchorage-independ cell growth as it occurs in soft agar can be used as an assay of cell tumorigenicity (*48*, *49*). We found, as a result of this genetic manipulation, more than 7-fold larger colony sizes for IBP knockdown clones in comparison to the control cells. Furthermore, our IBP knockdown clones produced more colonies and more cells per colony. These data are in corroboration with our previous studies on MA10 Leydig cells (*21*, *49*). It would be appropriate for us to extend the present observations by introducing these IBP knockdown clones into isogenic rats to monitor tumor development in vivo in comparison to grafts of control cells.

Our present experiments also showed that IBP knockdown clones show lower apoptotic levels and larger cell counts than control cells. Moreover, knockdown of IBP appeared to reduce the C6 glioma cells' sensitivity for the apoptosis inducing antineoplastic agent, ErPC, and its congener, ErPC3. The effect of PBR ligands on apoptosis is often considered to operate via interactions between mitochondrial IBP and VDAC (*61*, *62*). It has been suggested that this pathway, leading from modulation of VDAC by PBR ligands to apoptosis, involves depolarization of the mitochondrial membrane potential, mitochondrial cytochrome *c* release, and activation of caspase 3 and caspase 9 (*48*, *63*−*65*). In the present study, we found that knockdown of IBP prevented caspase 3 activation typically caused by the application of ErPC (*50*−*52*). This suggests that indeed the IBP component of the PBR complex is essential for activation of the apoptosis cascade running via cytochrome *c* release and caspase 3 and caspase 9 activation. On the other hand, IBP modulation of steroidogenesis has been well-studied and does not seem to require VDAC (*17*, *18*, *21*, *58*, *66*). In particular, 18 kDa IBP knockdown appears to reduce steroid production in MA10 Leydig cells (*21*). Interestingly, several studies have suggested that steroids may induce programmed cell death in C6 glioma cells (*67*, *68*). Steroids, such as progesterone, have also been found to induce apoptosis in other types of cancer cells (*69*, *70*). Furthermore, pregnenolone-sulfate has been shown to induce apoptosis in retinal cells (*71*). It would be interesting to study whether enhanced steroid production, including pregnenolone, due to PBR stimulation in tumorigenic cells, may activate these putative steroid-related apoptotic pathways.

As the knockdown vector of the present study was not selectively directed to mitochondrial PBR expression only, the expression of 18-kDa IBP may also have been affected in other cellular milieus (Tables 1, 2, and 5). While the majority of intracellular PBR typically is considered to be

present on the external mitochondrial membrane (*6*), PBR expression was also detected in nuclear, microsomal, and cytosomal fractions (*72*). Hardwick et al. (*73*) suggested that increased perinuclear/nuclear localization of IBP may occur in malignant breast tissues, where its main function may be to influence cell proliferation (*71*). In a previous study, we found that IBP knockdown did not affect the cellular proliferation rate (*21*), while the present and another previous study by us (*48*) suggest that the effect of IBP knockdown on C6 cell number is primarily modulated via apoptosis. It would be of interest in future genetic manipulation studies of cellular PBR to study the phenotype of cells presenting IBP overexpression specifically in selected cell organelles.

The majority of PBR protein in the mitochondrial membrane is found in complex with many other proteins, which are involved in different biological processes of cells, including apoptosis, steroidogenesis, proliferation, and oxidative phosphorylation. It is possible that PBR-related apoptosis may serve as a mechanism directed to regulate uncontrolled tumorigenic cell proliferation. To attain this PBR-related apoptosis, tumorigenic cells may increase their PBR expression (*48*). The suppression of such increase in PBR expression by our stable IBP antisense knockdown apparently enhanced the rate of the pathological proliferation of C6 cells, resulting in enhanced cell numbers (Figures 3 and 4). Interestingly, the IBP knockdown cells of our study even are able to sustain 25% more cells in cultures confluent for more than 4 days. Possibly, these cells lose some of their contact inhibition or are less sensitive to reduced availability of nutrients and oxygen due to crowding. Delay or reduction of PBR-related apoptosis may be an important factor for the regulation of cell proliferation following our antisense knockdown of IBP. Nonetheless, according to our previous study (*48*), high levels of PBR ligand binding density in unmanipulated C6 cells still does not allow adequate control on the cell proliferation. This indicates that an upregulation of PBR by itself in cancer cells is not sufficient to downregulate the cells' proliferation to normal levels. Nonetheless, our study suggests that upregulation of PBR, as observed in untreated cancer cells, may make such cancer cells more sensitive to antineoplastic agents, including ErPC and ErPC3.

In conclusion, our data suggest that increased cell proliferation in IBP knockdown cells is due to a loss of PBR-related apoptosis. This suggests that enhanced expression of IBP in tumorigenic cells may be a cellular mechanism to slow pathological proliferation of these transformed cells. Furthermore, our present study provides one of the first data that suggests a direct association between PBR expression and change in the cellular transformation level of cancer cells.

ACKNOWLEDGMENT

We thank Prof. H. Eibl, Max-Planck-Institut für biophysikalische Chemie, Göttingen, Germany, for letting us have the Erucylphosphocholine (ErPC) and its congener erucylphospho-*N*,*N*,*N*-trimethylammonium (ErPC3) prepared in his laboratory. We thank Vicky Kuznetsov for her help with the preparation of the manuscript.

REFERENCES

1. McEnery, M. W., Snowman, A. M., Trifiletti, R. R., and Snyder, S. H. (1992) Isolation of the mitochondrial benzodiazepine receptor: association with the voltage-dependent anion channel and the adenine nucleotide carrier, *Proc. Natl. Acad. Sci. U.S.A. 89*, 3170−3174.
2. Braestrup, C., and Squires, R. F. (1977) Specific benzodiazepine receptors in rat brain characterized by high-affinity [^{3}H]diazepam binding, *Proc. Natl. Acad. Sci. U.S.A. 74*, 3805−3809.
3. Verma, A., and Snyder, S. H. (1989) Peripheral type benzodiazepine receptors, *Annu. Rev. Pharmacol. Toxicol. 29*, 307−322.
4. Syapin, P. J., and Skolnick, P. (1979) Characterization of benzodiazepine binding sites in cultured cells of neural origin, *J. Neurochem. 32*, 1047−1051.
5. Schoemaker, H., Boles, R. G., Horst, W. D., and Yamamura, H. I. (1983) Specific high-affinity binding sites for [^{3}H]Ro 5-4864 in rat brain and kidney, *J. Pharmacol. Exp. Ther. 225*, 61−69.
6. Anholt, R. R. H., Pedersen, P. L., De Souza, E. B., and Snyder, S. H. (1986) The peripheral-type benzodiazepine receptor: localization to the mitochondrial outer membrane, *J. Biol. Chem. 261*, 576−583.
7. Antkiewicz-Michaluk, L., Guidotti, A., and Krueger, K. E. (1988a) Molecular characterization and mitochondrial density of a recognition site for peripheral-type benzodiazepine ligands, *Mol. Pharmacol. 34*, 272−278.
8. Antkiewicz-Michaluk, L., Mukhin, A. G., Guidotti, A., and Krueger, K. E. (1988b) Purification and characterization of a protein associated with peripheral-type benzodiazepine binding sites, *J. Biol. Chem. 263*, 17317−17321.
9. Mukherjee, S., and Das, S. K. (1989) Subcellular distribution of "peripheral type" binding sites for [^{3}H]Ro5-4864 in guinea pig lung. Localization to the mitochondrial inner membrane, *J. Biol. Chem. 264*, 16713−16718.
10. Papadopoulos, V., Boujrad, N., Ikonomovic, M. D., Ferrara, P., and Vidic, B. (1994) Topography of the Leydig cell mitochondrial peripheral-type benzodiazepine receptor, *Mol. Cell. Endocrinol. 104*, R5−9.
11. Culty, M., Li, H., Boujrad, N., Amri, H., Vidic, B., Bernassau, J. M., Reversat, J. L., and Papadopoulos, V. (1999) In vitro studies on the role of the peripheral-type benzodiazepine receptor in steroidogenesis, *J. Steroid Biochem. Mol. Biol. 69*, 123−130.
12. Golani, I., Weizman, A., Leschiner, S., Spanier, I., Eckstein, N., Limor, R., Yanai, J., Weisinger, G., and Gavish, M. (2001) Hormonal regulation of peripheral benzodiazepine receptor binding properties is mediated by subunit interaction, *Biochemistry 40*, 10213−10222.
13. Veenman, L., Leschiner, S., Spanier, I., Weisinger, G., Weizman, A., and Gavish, M. (2002) PK11195 attenuates kainic acid-induced seizures and alterations in peripheral-type benzodiazepine receptor (PBR) components in the rat brain, *J. Neurochem. 80*, 917−927.
14. Papadopoulos, V., Dharmarajan, A. M., Li, H., Culty, M., Lemay, M., and Sridaran, R. (1999) Mitochondrial peripheral-type benzodiazepine receptor expression. Correlation with gonadotropin-releasing hormone (GnRH) agonist-induced apoptosis in the corpus luteum, *Biochem. Pharmacol. 58*, 1389−1393.
15. Tsujimoto, Y., and Shimizu, S. (2000) VDAC regulation by the Bcl-2 family of proteins, *Cell Death Differ. 7*, 1174−1181.
16. Dolder, M., Wendt, S., and Wallimann, T. (2001) Mitochondrial creatine kinase in contact sites: interaction with porin and adenine nucleotide translocase, role in permeability transition and sensitivity to oxidative damage, *Biol. Signals Recept. 10*, 93−111.
17. Papadopoulos, V., Guarneri, P., Krueger, K. E., Guidotti, A., and Costa, E. (1992) Pregnenolone biosynthesis in C6 glioma cell mitochondria: regulation by diazepam-binding inhibitor mitochondrial receptor, *Proc. Natl. Acad. Sci. U.S.A. 89*, 5118−5122.
18. Papadopoulos, V., Amri, H., Boujrad, N., Cascio, C., Culty, M., Garnier, M., Hardwick, M., Li, H., Vidic, B., Brown, A. S., Reversa, J. L., Bernassau, J. M., and Drieu, K. (1997) Peripheral benzodiazepine receptor in cholesterol transport and steroidogenesis, *Steroids 62*, 21−28.
19. Weizman, R., Dagan, E., Snyder, S. H., and Gavish, M. (1997) Impact of pregnancy and lactation on $GABA_A$ receptor and central-type and peripheral-type benzodiazepine receptors, *Brain Res. 752*, 307−314.
20. Weizman, R., Leschiner, S., Schlegel, W., and Gavish, M. (1997) Peripheral-type benzodiazepine receptor ligands and serum steroid hormones, *Brain Res. 772*, 203−208.
21. Kelly-Hershkovitz, E., Weizman, R., Spanier, I., Leschiner, S., Lahav, M., Weisinger, G., and Gavish, M. (1998) Effects of peripheral-type benzodiazepine receptor antisense knockout on MA-10 Leydig cell proliferation and steroidogenesis, *J. Biol. Chem. 273*, 5478−5483.

22. Wang, J. K. T., Morgan, J. I., and Spector, S. (1984) Benzodiazepines that bind at peripheral sites inhibit cell proliferation, *Proc. Natl. Acad. Sci. U.S.A. 81*, 753−756.
23. Landau, M., Weizman, A., Zoref-Shani, E., Beery, E., Wasseman, L., Landau, O., Gavish, M., Brenner, S., and Nordenberg, J. (1998) Antiproliferative and differentiating effects of benzodiazepine receptor ligands on B16 melanoma cells, *Biochem. Pharmacol. 56*, 1029−1034.
24. Nordenberg, J., Fenig, E., Landau, M., Weizman, R., and Weizman, A. (1999) Effect of psychotropic drugs on cell proliferation and differentiation, *Biochem. Pharmacol. 58*, 1229−1236.
25. Carmel, I., Fares, F. A., Leschiner, S., Scherubl, H., Weisinger, G., and Gavish, M. (1999) Peripheral-type benzodiazepine receptors in the regulation of proliferation of MCF-7 human breast carcinoma cell line, *Biochem. Pharmacol. 58*, 273−278.
26. Hirsch, J. D., Beyer, C. F., Malkowitz, L., Beer, B., and Blume, A. J. (1989) Mitochondrial benzodiazepine receptors mediate inhibition of mitochondrial respiratory control, *Mol. Pharmacol. 35*, 157−163.
27. Zisterer, D. M., Gorman, A. M., Williams, D. C., and Murphy, M. P. (1992) The effects of the peripheral-type benzodiazepine acceptor ligands, Ro 5-4864 and PK 11195, on mitochondrial respiration, *Methods Find. Exp. Clin. Pharmacol. 14*, 85−90.
28. Ruff, M. R., Pert, C. B., Weber, R. J., Wahl, L. M., Wahl, S. M., and Paul, S. M. (1985) Benzodiazepine receptor-mediated chemotaxis of human monocytes, *Science 229*, 1281−1283.
29. Bessler, H., Caspi, B., Gavish, M., Rehavi, M., and Weizman, A. (1997) Significant inhibition of spontaneous IgA secretion by selective peripheral-type benzodiazepine receptor ligands, *Clin. Neuropharmacol. 20*, 215−223.
30. Krueger, K. E. (1995) Molecular and functional properties of mitochondrial benzodiazepine receptors, *Biochim. Biophys. Acta 1241*, 453−470.
31. Weizman, R., Burgin, R., and Gavish, M. (1993) Modulatory effect of antidepressants on peripheral-type benzodiazepine receptors, *Eur. J. Pharmacol. 250*, 289−294.
32. Avital, A., Richter-Levin, G., Leschiner, S., Spanier, I., Veenman, L., Weizman, A., and Gavish, M. (2001) Acute and repeated swim stress effects on peripheral benzodiazepine receptors in the rat hippocampus, adrenal, and kidney, *Neuropsychopharmacology 25*, 669−678.
33. Miyazawa, N., Diksic, M., and Yamamoto, Y. (1995) Chronological study of peripheral benzodiazepine binding sites in the rat brain stab wounds using [^{3}H]PK-11195 as a marker for gliosis, *Acta Neurochir. 137*, 207−216.
34. Veenman, L., and Gavish, M. (2000) Peripheral-type benzodiazepine receptors: their implication in brain disease, *Drug Dev. Res. 50*, 355−370.
35. Pubill, D., Verdaguer, E., Canudas, A. M., Sureda, F. X., Escubedo, E., Camarasa, J., Pallas, M., and Camins, A. (2001) Orphenadrine prevents 3-nitropropionic acid-induced neurotoxicity in vitro and in vivo, *Br. J. Pharmacol. 132*, 693−702.
36. Gavish, M., Bachman, I., Shoukrun, R., Katz, Y., Veenman, L., Weisinger, G., and Weizman, A. (1999) Enigma of the peripheral benzodiazepine receptor, *Pharmacol. Rev. 51*, 629−650.
37. Richfield, E. K., Ciliax, B. J., Starosta-Rubinstein, S. R., McKeever, P. E., Penney, J. B., and Young, A. B. (1988) Comparison of [^{14}C]-deoxyglucose metabolism and peripheral benzodiazepine receptor binding in rat C_6 glioma, *Neurology 38*, 1255−1262.
38. Ikezaki, K., Black, K. L., Santori, E. M., Smith, M. L., Becker, D. P., Payne, B. A., and Toga, A. W. (1990) Three-dimensional comparison of peripheral benzodiazepine binding and histological findings in rat brain tumor, *Neurosurgery 27*, 78−82.
39. Kletsas, D., Li, W., Han, Z., and Papadopoulos, V. (2004) Peripheral-type benzodiazepine receptor (PBR) and PBR drug ligands in fibroblast and fibrosarcoma cell proliferation: role of ERK, c-Jun and ligand-activated PBR-independent pathways, *Biochem. Pharmacol. 67*, 1927−1932.
40. Ferrarese, C., Appollonio, I., Frigo, M., Gaini, S. M., Piolti, R., and Frattola, L. (1989) Benzodiazepine receptors and diazepam-binding inhibitor in human cerebral tumors, *Ann. Neurol. 26*, 564−568.
41. Black, K. L., Ikezaki, K., Santori, E., Becker, D. P., and Vinters, H. V. (1990) Specific high-affinity binding of peripheral benzodiazepine receptor ligands to brain tumors in rat and man, *Cancer 65*, 93−97.
42. Marcian, E., Van Dort, M. E., Ciliax, B. J., Gildersleeve, D. L., Sherman, P. S., Rosenspire, K. C., Young, A. B., Junck, L., and Wieland, D. M. (1988) Radioiodinated benzodiazepines: agents for mapping glial tumors, *J. Med. Chem. 31*, 2081−2086.
43. Takada, A., Mitsuka, S., Diksic, M., and Yamamoto, Y. L. (1992) Autoradiographic study of peripheral benzodiazepine receptors in animal brain tumor models and human gliomas, *Eur. J. Pharmacol. 228*, 131−139.
44. Olson, J. M., Junck, L., Young, A. B., Penney, J. B., and Mancini, W. R. (1988) Isoquinoline and peripheral-type benzodiazepine binding in gliomas: implications for diagnostic imaging, *Cancer Res. 48*, 5837−5841.
45. Miyazawa, N., Hamel, E., and Diksic, M. (1998) Assessment of the peripheral benzodiazepine receptors in human gliomas by two methods, *J. Neuro−Oncol. 38*, 19−26.
46. Shiraishi, T., Black, K. L., Ikezaki, K., and Becker, D. P. (1991) Peripheral benzodiazepine induces morphological changes and proliferation of mitochondria in glioma cells, *J. Neurosci. Res. 30*, 463−474.
47. Ikezaki, K., and Black, K. L. (1990) Stimulation of cell growth and DNA synthesis by peripheral benzodiazepine, *Cancer Lett. 49*, 115−120.
48. Veenman, L., Levin, E., Weisinger, G., Leschiner, S., Spanier, I., Snyder, S. H., Weizman, A., and Gavish, M. (2004) Peripheral-type benzodiazepine receptor density and in vitro tumorigenicity of glioma cell lines, *Biochem. Pharm. 68*, 689−698.
49. Weisinger, G., Kelly-Hershkovitz, E., Veenman, L., Spanier, I., Leschiner, S., and Gavish, M. (2004) Peripheral benzodiazepine receptor antisense knockout increases tumorigenicity of MA-10 Leydig cells in vivo and in vitro, *Biochemistry 43*, 12315−12321.
50. Jendrossek, V., Erdlenbruch, B., Hunold, A., Kugler, W., Eibl, H., and Lakomek, M. (1999) Erucylphosphocholine, a novel antineoplastic ether lipid, blocks growth and induces apoptosis in brain tumor cell lines in vitro, *Int. J. Oncol. 14*, 15−22.
51. Jendrossek, V., Kugler, W., Erdlenbruch, B., Eibl, H., Lang, F., and Lakomek, M. (2001) Erucylphosphocholine-induced apoptosis in chemoresistant glioblastoma cell lines: involvement of caspase activation and mitochondrial alterations, *Anticancer Res. 21*, 3389−3396.
52. Kugler, W., Erdlenbruch, B., Jünemann, A., Heinemann, D., Eibl, H., and Lakomek, M. (2002) Erucylphosphocholine-induced apoptosis in glioma cells: involvement of death receptor signaling and caspase activation, *J. Neurochem. 82*, 1160−1170.
53. Gorman, C. M., Moffat, L. F., and Howard, B. H. (1982) Recombinant genomes which express chloramphenicol acetyltransferase in mammalian cells, *Mol. Cell Biol. 2*, 1044−1051.
54. Bradford, M. M. (1976) A rapid and sensitive method for the quantitation of microgram quantities of protein utilizing the principle of protein-dye binding, *Anal. Biochem. 72*, 248−54.
55. Awad, M., and Gavish, M. (1987) Binding of [^{3}H]Ro 5-4864 and [^{3}H]PK 11195 to cerebral cortex and peripheral tissues of various species: species differences and heterogeneity in peripheral benzodiazepine binding sites, *J. Neurochem. 49*, 1407−1414.
56. Vindelov, L. L., Christensen, I. J., and Nissen, N. I. (1983) A detergent-trypsin method for the preparation of nuclei for flow cytometric DNA analysis, *Cytometry 3*, 323−327.
57. Zar, J. M. (1974) *Biostatistical Analysis*, pp 101−162, Prentice-Hall, Englewood Cliffs, NJ.
58. Lacapere, J. J., and Papadopoulos, V. (2003) Peripheral-type benzodiazepine receptor: structure and function of a cholesterol-binding protein in steroid and bile acid biosynthesis, *Steroids 68*, 569−585.
59. Katz, Y., Ben-Baruch, G., Kloog, Y., Menczer, J., and Gavish, M. (1990) Increased density of peripheral benzodiazepine-binding sites in ovarian carcinomas as compared with benign ovarian tumours and normal ovaries, *Clin. Sci. 78*, 155−158.
60. Katz, Y., Eitan, A., and Gavish M. (1990) Increase in peripheral benzodiazepine binding sites in colonic adenocarcinoma, *Oncology 47*, 139−142.
61. Verrier, F., Mignotte, B., Jan, G., and Brenner, C. (2003) Study of PTPC composition during apoptosis for identification of viral protein target, *Ann. N.Y. Acad. Sci. 1010*, 126−142.
62. Kunduzova, O. R., Escourrou, G., De La Farge, F., Salvayre, R., Seguelas, M. H., Leducq, N., Bono, F., Herbert, J. M., and Parini, A. (2004) Involvement of peripheral benzodiazepine receptor in the oxidative stress, death-signaling pathways, and renal injury induced by ischemia-reperfusion, *J. Am. Soc. Nephrol. 15*, 2152−2160.
63. Maaser, K., Hopfner, M., Jansen, A., Weisinger, G., Gavish, M., Kozikowski, A. P., Weizman, A., Carayon, P., Riecken, E. O., Zeitz, M., and Scherubl, H. (2001) Specific ligands of the

peripheral benzodiazepine receptor induce apoptosis and cell cycle arrest in human colorectal cancer cells, *Br. J. Cancer. 85*, 1771−1780.

64. Chelli, B., Lena, A., Vanacore, R., Pozzo, E. D., Costa, B., Rossi, L., Salvetti, A., Scatena, F., Ceruti, S., Abbracchio, M. P., Gremigni, V., and Martini, C. (2004) Peripheral benzodiazepine receptor ligands: mitochondrial transmembrane potential depolarization and apoptosis induction in rat C6 glioma cells, *Biochem. Pharmacol. 68*, 125−134.
65. Jorda, E. G., Jimenez, A., Verdaguer, E., Canudas, A. M., Folch, J., Sureda, F. X., Camins, A., and Pallas, M. (2005) Evidence in favour of a role for peripheral-type benzodiazepine receptor ligands in amplification of neuronal apoptosis, *Apoptosis. 10*, 91−104.
66. Gavish, M., and Weizman, R. (1997) Role of peripheral-type benzodiazepine receptors in steroidogenesis, *Clin. Neuropharmacol. 20*, 473−481.
67. Baudet, C., Chevalier, G., Chassevent, A., Canova, C., Filmon, R., Larra, F., Brachet, P., and Wion, D. (1996) 1,25-Dihydroxyvitamin D3 induces programmed cell death in a rat glioma cell line, *J. Neurosci. Res. 46*, 540−550.
68. Elias, J., Marian, B., Edling, C., Lachmann, B., Noe, C. R., Rolf, S. H., and Schuster, I. (2003) Induction of apoptosis by vitamin D metabolites and analogs in a glioma cell line, *Recent Results Cancer Res. 164*, 319−332.
69. Ansquer, Y., Legrand, A., Bringuier, A. F., Vadrot, N., Lardeux, B., Mandelbrot, L., and Feldmann, G. (2005) Progesterone induces BRCA1 mRNA decrease, cell cycle alterations and apoptosis in the MCF7 breast cancer cell line, *Anticancer Res. 25*, 243−248.
70. Syed, V., Mukherjee, K., Lyons-Weiler, J., Lau, K. M., Mashima, T., Tsuruo, T., and Ho, S. M. (2005) Identification of ATF-3, caveolin-1, DLC-1, and NM23-H2 as putative antitumorigenic, progesterone-regulated genes for ovarian cancer cells by gene profiling, *Oncogene 24*, 1774−1787.
71. Cascio, C., Guarneri, R., Russo, D., De Leo, G., Guarneri, M., Piccoli, F., and Guarneri, P. (2002) A caspase-3-dependent pathway is predominantly activated by the excitotoxin pregnenolone sulfate and requires early and late cytochrome *c* release and cell-specific caspase-2 activation in the retinal cell death, *J. Neurochem. 83*, 1358−1371.
72. Alenfall, J., d'Argy, R., and Batra, S. (1994) Whole-body autoradiografic study of [^{3}H]-PK 11195 distribution in dunning AT-1 tumor-bearing rats, *Oncol. Res. 6*, 603−609.
73. Hardwick, M., Fertikh, D., Culti, M., Li, H., Vidic, B., and Papadopoulos, V. (1999) Peripheral-type benzodiazepine receptor (PBR) in human breast cancer: correlation of breast cancer cell aggressive phenotype with PBR expression, nuclear localization, and PBR-mediated cell proliferation and nuclear transport of cholesterol, *Cancer Res. 59*, 831−842.
74. Brown, R. C., Degenhardt, B., Kotoula, M., and Papadopoulous, V. (2000) Location-dependent role of the human glioma cell peripheral-type benzodiazepine receptor in proliferation and steroid biosynthesis, *Cancer Lett. 156*, 125−132.

BI050150S